ARCHIVE OF MECHANICAL ENGINEERING

VOL. LXV 2018 Number 4

DOI: 10.24425/ame.2018.125438

Key words: railway vehicle, flexible carbody, suspended equipment, bending vibration, ride comfort

MĂDĂLINA DUMITRIU[1]

NUMERICAL ANALYSIS ON THE INFLUENCE OF SUSPENDED EQUIPMENT ON THE RIDE COMFORT IN RAILWAY VEHICLES

To study the impact of suspended equipment on the ride comfort in a railway vehicle, a rigid flexible general model of such a vehicle is required. The numerical simulations is based on two different models, derived from the general model of the vehicle, namely a reference model of a vehicle with no equipment, and another model with six suspended elements of equipment mounted in various positions along the carbody. The objective of this paper arises from the observation that the literature does not contain any study that highlights the change in the ride comfort resulting exclusively due to the influence of equipment. The influence of the suspended equipment on the ride comfort is determined by comparing the ride comfort indices calculated in the carbody reference points, at the centre and above the two bogies, for a model with six elements of equipment and a model of the vehicle with no equipment.

1. Introduction

One of the basic criteria taken into account in designing the high-speed railway vehicles is the reduction in the vehicle weight, particularly of the carbody that is the most relevant component for the total vehicle mass. A lighter weight of the vehicle brings a significant contribution to a higher speed, lower energy consumption, reduction in the ground vibration and construction-cost saving [1, 2].

The design aimed at carbody weight lightening implies the use of light materials and altering mechanical structures [3], which often leads to a lower carbody structural stiffness and, therefore, a decrease of the eigenfrequencies. The lighter the vehicle carbody, the higher its flexibility, which results in easy excitation of the carbody structural vibrations that have a negative effect on the ride comfort. Similarly, the structural vibration leads to carbody fatigue, which affects the dynamic performances and decreases the service life of the vehicle [4].

[1] *Department of Railway Vehicles, University Politehnica of Bucharest, Bucharest, Romania. Email: madalinadumitriu@yahoo.com*

www.czasopisma.pan.pl PAN POLSKA AKADEMIA NAUK www.journals.pan.pl

The carbody structural vibration is rather complex, with global and local mode shapes that include carbody bending, torsion to the roof, floor, side and walls vibration [5]. Nevertheless, the highest influence on the ride comfort originates from the first carbody eigenmode of vertical bending – the symmetrical bending, whose frequency can fall into the range of 6 to 12 Hz where the human body shows a greater sensitivity to vertical vibrations.

The problem of suppression of the carbody flexible vibration in the railway vehicles has become a priority for the academic research studies. In recent years, in the literature one can find more articles on the possibility of reducing the carbody vertical vibration of the high-speed electric multiple units (EMU). For the purpose of lightweight design of the vehicle system, one needs to scale down the layout of the doors and air conditioning installation holes, the carbody stiffness and the modal frequency. This might deteriorate suppression of the flexible vibration of the carbody and affect the ride comfort [6].

Many elements of functional equipment are directly suspended under the carbody underframe, including the traction transformer, the traction converter, the braking unit, the cooling unit, the air compressor, and the waste collection unit. The weight of such devices can vary from several tens of kilograms to tones and some of them, namely the cooling fan and the mechanical switch, may have their own sources of vibrations. The design of the EMU has a significant influence on the carbody vertical bending frequency. Depending on the suspension system, the equipment mass and its mounting position, the first frequency corresponding to the flexible vibration mode of the carbody – equipment coupled system can decrease and reach the interval where the human body is more sensitive.

In general, the elements of equipment are elastically suspended, using rubber springs, in order to prevent noise transmission and to lower the level of carbody vibration so that the ride comfort is not significantly affected. However, the quest for the best solution for equipment suspension is still at the centre of numerous studies. Many of them focus on the relation between the parameters of the equipment suspension, i.e., the equipment eigenfrequency and the frequency of the first carbody vertical bending mode, in correlation with the equipment mass and its mounting position [2, 3, 7–10]. In all cases, the results confirm that the frequency of suspended equipment elements should be sufficiently low and the equipment should have the largest possible mass and be mounted closest to the carbody centre, in order to obtain a significant reduction in the carbody flexible vibration. There are also studies suggesting new methods of designing the equipment suspension [3, 11] or new solutions for this suspension requiring the use of high-damping elastic support [12].

According to different design concepts, there are two conventional methods to reduce the carbody flexible vibrations: EMU – vibration isolation, and dynamic vibration absorber (DVA) to which the active reduction of the vibrations can be added, yet not applicable due to its high costs, difficulty to maintain and limited space of the equipment cabin [11]. The vibration isolation system is placed between

www.czasopisma.pan.pl PAN POLSKA AKADEMIA NAUK www.journals.pan.pl

the equipment and the carbody underframe, where the capability of transmission of force or the displacement between the equipment and the carbody can be reduced. For instance, Shi et al. [13] took into account a single stage and two-stage vibration isolation system, respectively, in order to study the vibration transmission characteristics of a flexible carbody and its suspended equipment. The carbody elastically suspended equipment can be looked at as a DVA, whose help counts in the control of the amplitude of the carbody flexible vibrations. The DVA theory was implemented by Huang et al. [2], Ye et al. [6] and Shi et al. [14], to attenuate the flexible vibration of the carbody for EMU. Based on DVA theory, Shi et al. [13, 15] calculated the optimal frequencies of the various suspended pieces of equipment. Sun et al. [11] suggest methods for the underframe equipment of a high-speed railway vehicle based on the DVA theory and vibration isolation theory, respectively.

To study the influence of the suspended equipment on the carbody flexible vibrations and on the ride comfort, a rigid-flexible coupled model is often used. It consists of the carbody modelled via an Euler–Bernoulli beam, a single suspended equipment element mounted at the carbody centre and rigid bodies for two bogies and four wheelsets, in which only the vertical vibration modes (i.e., bounce, pitch and flexible bending modes) influencing the vertical ride comfort are taken into account [2, 8, 14, 16]. A more complex representation of the carbody would use 3D rigid-flexible coupled models built in compliance with the multibody system (MBS) theory and the finite element method (FEM) [3, 6, 7, 14, 17]. In reality, there are more suspended equipment elements mounted under the EMU underframe, as shown above. There are a few studies that consider all these equipment elements and use 3D rigid-flexible coupled models in line with the MBS theory and the finite element method (FEM). For instance, Sun et al. [3] built a 3D model with FE software HYPERMESH, in which an electro-pneumatic brake unit, charger, inverter, and battery system were included. Shi et al. [14, 18] set up a 3D rigid-flexible coupled vehicle system dynamics model for a passenger coach of EMU by ANSYS and SIMPACK where six elements of equipment were mounted on the underframe, namely the traction transformer, the traction converter, the braking unit, the power inverter, the waste discharge unit, and the effluent tank.

However, as mentioned above, the literature does not include any studies highlighting the change of the ride comfort exclusively due to the influence of equipment. This observation is the starting point for the paper herein.

The paper brings into attention the impact of the equipment itself on the ride comfort in order to better understand the vibration behaviour of such vehicles, and to help in this way the designers to improve the ride comfort of a high-speed vehicle. The paper aims at conducting a numerical analysis of the impact that the suspended equipment has on the ride comfort evaluated by the ride comfort index calculated in three reference points of the carbody – at the centre and above the two bogies. To this end, a general coupled rigid – flexible model is considered, which

www.czasopisma.pan.pl PAN POLSKA AKADEMIA NAUK www.journals.pan.pl

includes a body with distributed parameters for the carbody, six rigid bodies for the bogies and wheelsets and more rigid bodies for the suspended equipment elements. To perform the numerical simulations, two models are derived from the vehicle's general model, namely a reference model of a vehicle with no equipment and a model considering six equipment elements installed in different positions along the carbody. The optimum rigidity and damping of the equipment suspension and, respectively, the optimum frequency, are calculated based on the DVA theory. In this study we intend to analyse the change in the ride comfort exclusively due to the suspended equipment; this is possible via a comparison between the results coming from the model with six elements of equipment with the results of the model with no equipment.

2. The general model of the vehicle

To study the influence that the suspended equipment exert on the ride comfort, a four-axle and two-stage suspension vehicle is considered, travelling at a constant velocity V on a track, deemed as perfectly rigid, with vertical irregularities. The irregularities of the track are described with respect to each axle via the functions η_j, with $j = 1, \ldots, 4$.

The vehicle is represented by a rigid-flexible coupled model (Fig. 1), used on a regular basis for such studies, thanks to the fact that it provides a good agreement between the numerical simulations and the field tests [2].

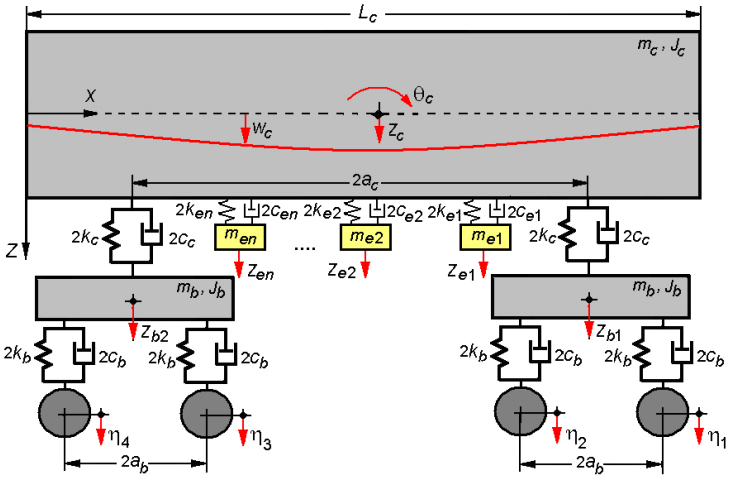

Fig. 1. Wing tip force vs. tip twist comparison

The model consists of a body with distributed parameters for the carbody and several rigid bodies for the bogies, axles and the suspended equipment. Both two stages of the suspension and the suspension system of the equipment are modelled

www.czasopisma.pan.pl PAN POLSKA AKADEMIA NAUK www.journals.pan.pl

via Kelvin–Voigt type systems. The parameters for the vehicle model are listed in Table 1.

Table 1.

Model parameters of the vehicle

Symbol	Definition	Symbol	Definition
m_c	Carbody mass	$2c_c$	Secondary suspension damping (per bogie)
m_b	Bogie suspended mass	$2k_c$	Secondary suspension stiffness (per bogie)
$m_{e1\ldots n}$	Equipment mass	$2c_b$	Primary suspension damping (per axle)
J_c	Carbody inertia moment	$2k_b$	Primary suspension stiffness (per axle)
J_b	Bogie inertia moment	$2c_{e1\ldots n}$	Suspension damping in pieces of equipment
L_c	Carbody length	$2k_{e1\ldots n}$	Suspension stiffness in pieces of equipment
$2a_c$	Carbody wheelbase	$2a_b$	Bogie wheelbase

The carbody is represented by a free-free equivalent beam, with constant section and uniformly distributed mass, of Euler–Bernoulli type. The beam parameters are defined in terms of the carbody elements, such as: L_c – beam length; $\rho_c = m_c/L_c$ – beam mass per length unit, where m_c is the carbody mass; μ – structural damping coefficient; EI – bending modulus, where E is the longitudinal modulus of elasticity, and I is the area moment of inertia of the beam transversal section.

The carbody rigid vibration modes – bounce z_c and pitch θ_c, and the first carbody bending eigenmode in a vertical plan will be taken into account.

The general form of the carbody equation of motion is

$$EI\frac{\partial^4 w_c(x,t)}{\partial x^4} + \mu I\frac{\partial^5 w_c(x,t)}{\partial x^4 \partial t} + \rho_c\frac{\partial^2 w_c(x,t)}{\partial t^2} = \sum_{i=1}^{2} F_{ci}\delta(x-l_i) + \sum_{k=1}^{n} F_{ek}\delta(x-l_{ek}) \tag{1}$$

where $\delta(.)$ is Dirac delta function, distances l_i (for $i = 1, 2$) fix the supporting points position of the carbody on the secondary suspension, while the distances l_{ek} (for $k = 1 \ldots n$) fix the supporting points position of the equipment elements on the vehicle carbody; F_{ci} stands for the forces derived from the secondary suspension corresponding to bogie i, whereas F_{ek} represents the forces coming from the suspension of the equipment elements (Fig. 2)

$$F_{ci} = -2c_c\left(\frac{\partial w_c(l_i,t)}{\partial t} - \dot{z}_{bi}\right) - 2k_c(w_c(l_i,t) - z_{bi}), \tag{2}$$

$$F_{ek} = -2c_{ek}\left[\frac{\partial w_c(l_{ek},t)}{\partial t} - \dot{z}_e\right] - 2k_{ek}\left[w_c(l_{ek},t) - z_{ek}\right]. \tag{3}$$

www.czasopisma.pan.pl PAN POLSKA AKADEMIA NAUK www.journals.pan.pl

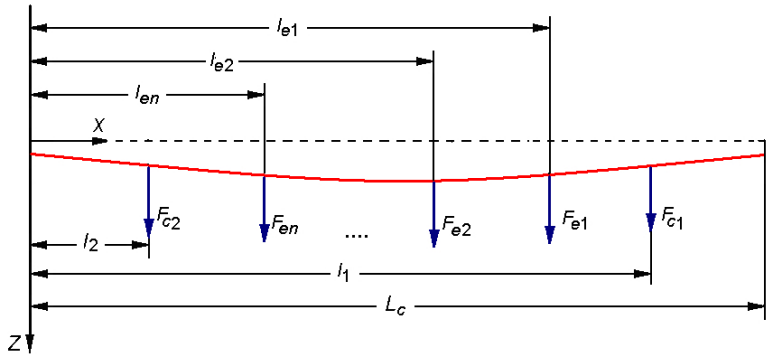

Fig. 2. Forces acting upon the carbody

The carbody vertical movement $w_c(x,t)$ origins from the superposition of the two rigid vibration modes – bounce and pitch, with the first bending mode

$$w_c(x,t) = z_c(t) + \left(x - \frac{L_c}{2}\right)\theta_c(t) + X_c(x)T_c(t), \tag{4}$$

where $T_c(t)$ is the time coordinate of the first bending eigenmode in a vertical plan and $X_c(x)$ stands for its eigenfunction

$$X_c(x) = \sin\beta x + \sinh\beta x - \frac{\sin\beta L_c - \sinh\beta L_c}{\cos\beta L_c - \cosh\beta L_c}(\cos\beta x + \cosh\beta x) \tag{5}$$

with

$$\beta = \sqrt[4]{\omega_c^2\rho_c/(EI)} \tag{6}$$

and

$$\cos\beta L_c \cosh\beta L_c - 1 = 0, \tag{7}$$

where ω_c is the natural angular frequency of the carbody bending.

When applying the modal analysis method and considering the orthogonality property of the eigenfunction in the carbody vertical bending, the equation of motion (1) turns into three two-order differential equations with ordinary derivatives, describing the movements of bounce, pitch and bending in the carbody:

$$m_c\ddot{z}_c = \sum_{i=1}^{2} F_{ci} + \sum_{k=1}^{n} F_{ek}\,, \tag{8}$$

$$J_c\ddot{\theta}_c = \sum_{i=1}^{2} F_{ci}\left(l_i - \frac{L_c}{2}\right) + \sum_{k=1}^{n} F_{ek}\left(l_{ek} - \frac{L_c}{2}\right), \tag{9}$$

$$m_{mc}\ddot{T}_c + c_{mc}\dot{T}_c + k_{mc}T_2 = \sum_{i=1}^{2} F_{ci}X_c(l_i) + \sum_{k=1}^{n} F_{ek}X_c(l_{ek}), \tag{10}$$

www.czasopisma.pan.pl PAN POLSKA AKADEMIA NAUK www.journals.pan.pl

where k_{mc}, c_{mc} and m_{mc} are stiffness, damping and the carbody modal mass given in the below equations

$$k_{mc} = EI\int_0^L \left(\frac{\mathrm{d}^2 X_c}{\mathrm{d}x^2}\right)^2 \mathrm{d}x, \quad c_{mc} = \mu I\int_0^L \left(\frac{\mathrm{d}^2 X_c}{\mathrm{d}x^2}\right)^2 \mathrm{d}x, \quad m_{mc} = \rho_c \int_0^L X_c^2 \,\mathrm{d}x. \tag{11}$$

For each bogie, a single mode of vibration is considered, namely the bounce z_{bi}, with $i = 1, 2$. The pitch movement of the bogie is neglected since it is not transmitted to the vehicle carbody in this model.

The equations for the bounce movements of the bogies are:

$$m_b \ddot{z}_{b1} = \sum_{j=1}^{2} F_{bj} - F_{c1}\,, \tag{12}$$

$$m_b \ddot{z}_{b2} = \sum_{j=3}^{4} F_{bj} - F_{c2}\,, \tag{13}$$

where F_{bj} stands for the forces coming from the primary suspension that correspond to axle j, as below

$$F_{b1,2} = -2c_b\,(\dot{z}_{b1} - \dot{\eta}_{1,2}) - 2k_b(z_{b1} - \eta_{1,2}), \quad \text{for } j = 1, 2, \tag{14}$$

$$F_{b3,4} = -2c_b\,(\dot{z}_{b2} - \dot{\eta}_{3,4}) - 2k_b(z_{b2} - \eta_{3,4}), \quad \text{for } j = 3, 4. \tag{15}$$

The suspended equipment elements make bounce movements that are described by the following equations:

$$m_{ek}\ddot{z}_{ek} = -\sum_{k=1}^{n} F_{ek}\,. \tag{16}$$

The system comprising the equations (8)–(10), (12), (13) and (16) can be written as matrices of the form

$$\mathbf{M}\ddot{\mathbf{p}} + \mathbf{C}\dot{\mathbf{p}} + \mathbf{K}\,\mathbf{p} = \mathbf{P}\dot{\boldsymbol{\eta}} + \mathbf{R}\boldsymbol{\eta}, \tag{17}$$

where **M**, **C** and **K** are the inertia, damping and stiffness matrices, and **P**, **R** are the track displacement and velocity input matrices. The motions of each body can be solved numerically using compiled MATLAB codes.

3. Numerical analysis

This section is concerned with the results of the numerical study regarding the influence that the suspended equipment has on the ride comfort, evaluated by the comfort index. Two distinct models of the vehicle derived from the general model in the previous section are applied – a reference model with no equipment and another model considering six elements of equipment – hereinafter called "model with no equipment" and, respectively "model with equipment".

www.czasopisma.pan.pl PAN POLSKA AKADEMIA NAUK www.journals.pan.pl

3.1. The parameters of the numerical model

The reference parameters of the numerical model are listed in Table 2, as determined for a motor vehicle of EMU exploited in high-speed railway transport of China [14]. The frequency of the vertical bending of the carbody with no equipment is $f_{vb} = 12.1$ Hz, while the frequencies of the carbody bounce and pitch are $f_{bc} = 1.25$ Hz and $f_{pc} = 1.5$ Hz, respectively. The frequency of the bogie bounce is $f_{bb} = 8.36$ Hz.

Table 2.

Parameters of the numerical model

$m_c = 26000$ kg	$2k_c = 1.2$ MN/m
$m_b = 2050$ kg	$2c_c = 29.97$ kNs/m
$J_c = 1600 \cdot 10^3$ kg m^2	$4k_b = 4.4$ MN/m
$J_b = 830$ kg m^2	$4c_b = 41.78$ kNs/m
$EI = 4.2554 \cdot 10^9$ N m^2	$m_{mc} = 26936$ kg
$L_c = 24.2$ m	$k_{mc} = 155.69$ MN/m
$2a_c = 17.375$ m; $2a_b = 2.5$ m	$c_{mc} = 61.437$ kNm/s

Six elements of equipment are suspended under the carbody underframe, mounted at different distances from the carbody end. The heaviest one weighs 3960 kg and the lightest 145 kg (see Table 3).

Table 3.

Mass and mounting position for the equipment

Equipment element	Equipment mass m_{ek} [kg]	Mounting position l_{ek} [m]	Mass ratio $u_k = m_{ek}/m_c$
Traction transformer	3960	12.8	0.1523
Traction converter	1675	7.2	0.0644
Braking unit	400	9.9	0.0153
Power inverter	540	15.3	0.0207
Waste discharge unit	145	23.2	0.0055
Effluent tank	720	0.75	0.0277

While considering that each of the six equipment elements acts like a DVA, the optimal stiffness and damping in the equipment suspension can be expressed as a function of the optimal tuning ratio ($\tau_{ek,\,\mathrm{opt}}$) and optimal damping ($\zeta_{ek,\,\mathrm{opt}}$), based on the relations [2], for $k = 1 \ldots 4$,

$$\tau_{ek,\,\mathrm{opt}} = \frac{1}{1 + u_k X_c^2(l_{ek})}, \tag{18}$$

$$\zeta_{ek,\,\mathrm{opt}} = \sqrt{\frac{3u_k X_c^2(l_{ek})}{8 + 8u_k X_c^2(l_{ek})}}. \tag{19}$$

Consequently, the optimal stiffness and damping in the equipment suspension can be expressed as below:

$$2k_{ek,\,\mathrm{opt}} = m_{ek}(2\pi f_{vb}\tau_{ek,\,\mathrm{opt}})^2\,, \tag{20}$$

$$2c_{ek,\,\mathrm{opt}} = \zeta_{ek,\,\mathrm{opt}}\left(2\sqrt{2k_{ek,\,\mathrm{opt}}m_{ek}}\right)\,. \tag{21}$$

Similarly, the optimal frequency of the equipment can be calculated, according to the relation

$$f_{ek,\,\mathrm{opt}} = f_{vb}\tau_{ek,\,\mathrm{opt}}\,. \tag{22}$$

The results from the above equations are included in Table 4. We can notice that the optimal damping has a value that is too high for the rubber elements normally used for the suspension systems of the equipment, where the damping ratio should not exceed 0.075. Otherwise, they will easily warm up, hence they will age and creep quickly [2]. Further in this the study we will apply a reference value of $\zeta_{ek} = \zeta_e = 0.025$.

Table 4.

Optimal stiffness and damping of the suspension system for the equipment

Equipment mass m_{ek} [kg]	Optimal tuning ratio $\tau_{ek,\,\mathrm{opt}}$	Optimal damping $\zeta_{ek,\,\mathrm{opt}}$	Optimal frequency $f_{ek,\,\mathrm{opt}}$ [Hz]
$m_{e1} = 145$	0.985	0.0747	11.92
$m_{e2} = 540$	0.982	0.0813	11.88
$m_{e3} = 3960$	0.814	0.2636	9.85
$m_{e4} = 400$	0.982	0.0820	11.88
$m_{e5} = 1675$	0.980	0.0828	11.87
$m_{e6} = 720$	0.922	0.1705	11.16

3.2. Ride comfort index

To evaluate the ride comfort, the influence of track irregularities is considered as a stationary stochastic process, which can be described via the power spectral density as in equation [19]

$$S(\Omega) = \frac{A\Omega_c^2}{(\Omega^2 + \Omega_r^2)(\Omega^2 + \Omega_c^2)}\,, \tag{23}$$

where Ω is the wavelength, $\Omega_c = 0.8246$ rad/m, $\Omega_r = 0.0206$ rad/m, and A is a coefficient depending on the track quality. For a high level quality track, $A = 4.032 \cdot 10^{-7}$ rad m, whereas for a low level quality the coefficient A is $1.080 \cdot 10^{-6}$ rad m.

www.czasopisma.pan.pl PAN POLSKA AKADEMIA NAUK www.journals.pan.pl

As a function of the angular frequency $\omega = V\Omega$, the power spectral density of the track irregularities can be written as in the general relation

$$G(\omega) = \frac{S(\omega/V)}{V}. \tag{24}$$

The equations (23) and (24) will give the power spectral density of the track vertical irregularities in the below form

$$G(\omega) = \frac{A\Omega_c^2 V^3}{[\omega^2 + (V\Omega_c)^2]\,[\omega^2 + (V\Omega_r)^2]}. \tag{25}$$

To calculate the power spectral density of the carbody vertical acceleration, the following relationship applies

$$G_{ac}(x,\omega) = G(\omega)\left|\overline{H}_{ac}(x,\omega)\right|^2, \tag{26}$$

where $\overline{H}_{ac}(x,\omega)$ represents the response function of the carbody acceleration at a random point x on the carbody longitudinal axis,

$$\overline{H}_{ac}(x,\omega) = \omega^2\left[\overline{H}_{z_c}(\omega) + \left(\frac{L_c}{2} - x\right)\overline{H}_{\theta_c}(\omega) + X_c(x)\overline{H}_{T_c}(\omega)\right], \tag{27}$$

where $\overline{H}_{z_c}(\omega)$, $\overline{H}_{\theta_c}(\omega)$, $\overline{H}_{T_c}(\omega)$ are the response functions corresponding to the rigid vibration modes – bounce and pitch (z_c and θ_c) and to the carbody vertical bending (T_c).

To calculate the response function, the track vertical irregularities against each axle are considered to be of a harmonic shape, with the wavelength Λ and amplitude η_0 and are de-phased against the axles corresponding to the distances between them, $2a_c$ and $2a_b$. Hence, the functions η_j describing the track irregularities against the four axles are in the form of

$$\eta_{1,2}(t) = \eta_0 \cos\omega\left(t + \frac{a_c \pm a_b}{V}\right), \qquad \eta_{3,4}(t) = \eta_0 \cos\omega\left(t - \frac{a_c \mp a_b}{V}\right). \tag{28}$$

where $\omega = 2\pi V/\Lambda$ represents the track excitation-induced pulsation.

When customizing the relation (27), we obtain the power spectral density of the acceleration at the carbody centre and above the two bogies as

$$G_{acm}(\omega) = G(\omega)\left|\overline{H}_{acm}(\omega)\right|^2, \tag{29}$$

$$G_{acb_i}(\omega) = G(\omega)\left|\overline{H}_{acb_i}(\omega)\right|^2. \tag{30}$$

To evaluate the comfort in the vertical direction, the partial comfort index is used, which is calculated with relation [20]

$$N_{MV} = 6a_{95}^{W_{ab}}, \tag{31}$$

where a is the root mean square of the vertical carbody acceleration, 95 refers to the quantile of order 95%, and $W_{ab} = W_a W_b$ represents the weight filter of the vertical acceleration [20, 21].

The root mean square of the vertical acceleration in a random point x of the carbody is calculated by using the carbody dynamic response, expressed as the acceleration power spectral density, in the equation below

$$a = \sqrt{\frac{1}{\pi}\int_0^\infty G_{ac}(x,\omega)\,\mathrm{d}\omega}. \tag{32}$$

Similarly, the root mean square of the acceleration at the carbody centre or above the bogies can be calculated using the relations

$$a_m = \sqrt{\frac{1}{\pi}\int_0^\infty G_{cam}(\omega)\,\mathrm{d}\omega}, \tag{33}$$

$$a_{b1,2} = \sqrt{\frac{1}{\pi}\int_0^\infty G_{acb1,2}(\omega)\,\mathrm{d}\omega}. \tag{34}$$

The filter W_a is a passband filter with the transfer function (Fig. 3a)

$$H_a(s) = \frac{s^2\,(2\pi f_2)^2}{\left[s^2 + \dfrac{2\pi f_1}{Q_1}s + (2\pi f_1)^2\right]\left[s^2 + \dfrac{2\pi f_2}{Q_1}s + (2\pi f_2)^2\right]}, \tag{35}$$

with $f_1 = 0.4$ Hz, $f_2 = 100$ Hz and $Q_1 = 0.71$ and $s = \mathrm{i}\omega$ (with $\mathrm{i}^2 = -1$) [21].

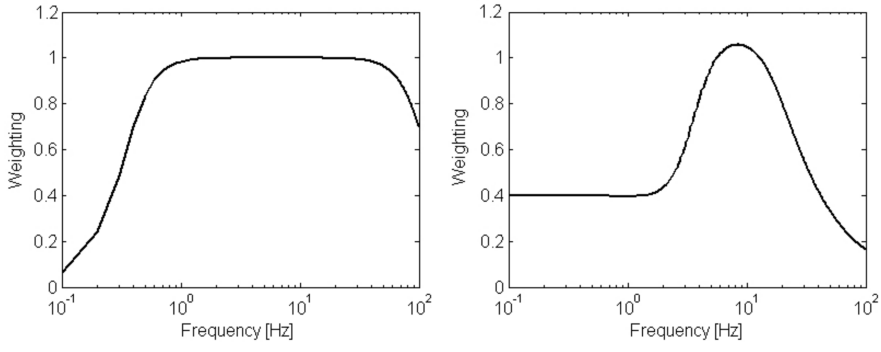

(a) (b)

Fig. 3. The transfer functions of the weighting filters: (a) filter W_a; (b) filter W_b

The weighting filter W_b takes into account the high human sensitivity to the vertical vibrations and has the transfer function in the form of (Fig. 3b)

$$H_b(s) = \frac{(s+2\pi f_3)\cdot\left[s^2+\dfrac{2\pi f_5}{Q_3}s+(2\pi f_5)^2\right]2\pi K f_4^2 f_6^2}{\left[s^2+\dfrac{2\pi f_4}{Q_2}s+(2\pi f_4)^2\right]\left[s^2+\dfrac{2\pi f_6}{Q_4}s+(2\pi f_6)^2\right]f_3 f_5^2}, \tag{36}$$

where $f_3 = 16$ Hz, $f_4 = 16$ Hz, $f_5 = 2.5$ Hz, $f_6 = 4$ Hz, $Q_2 = 0.63$, $Q_4 = 0.8$, $K = 0.4$ and $s = \mathrm{i}\omega$ (with $\mathrm{i}^2 = -1$) [21].

When we accept the hypothesis that the vertical accelerations have a Gaussian distribution with zero mean value, the partial comfort index can be derived from

$$N_{MV}(x) = 6\Phi^{-1}(0.95)\sqrt{\frac{1}{\pi}\int_0^\infty G_{ac}(x,\omega)\,|H_{ab}(\omega)|^2\,\mathrm{d}\omega}, \tag{37}$$

where $\Phi^{-1}(0.95)$ represents the quantile of the standard Gaussian distribution with the probability of 95%, and the transfer function $H_{ab}(\omega) = H_a(\omega)H_b(\omega)$ (Fig. 4).

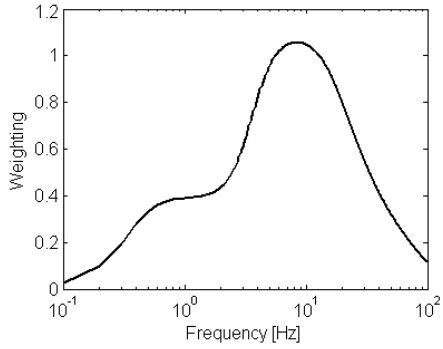

Fig. 4. The transfer functions of the W_{ab} filter

To calculate the comfort index at the carbody centre (N_{MVm}) and above the two bogies ($N_{MVb1,2}$), the particular relations (29) and (30) of the acceleration power spectral density are considered.

3.3. Numerical simulations results

In this section, based on the numerical simulation results, we analyse the influence of the equipment on the ride comfort, in correlation with velocity and different values of the bending frequency f_{vb} ranging from 7 to 13 Hz. To this end, the ride comfort index will be calculated at the carbody centre and above the two bogies, based on the model with equipment and the results will be then compared

www.czasopisma.pan.pl PAN POLSKA AKADEMIA NAUK www.journals.pan.pl

to the ones derived from the model with no equipment. This will give a real image of the contribution that the equipment elements bring in the change of the ride comfort.

The diagrams in Fig. 5 show the ride comfort index at the carbody centre. A first general observation is that the comfort index increases along with the velocity, irrespective of the applied model, but this increase is not uniform, due to the geometric filtering effect. The geometric filtering effect is an essential feature of the behaviour of vertical vibrations in the railway vehicles, extensively analysed in many papers [22–27]. This effect is mainly due to the manner in which the track excitations are conveyed to the suspended masses via the axles, irrespective of the suspension characteristics. In essence, the geometric filtering effect is the result of the displacement between the vertical movements in the axles that appear as the car runs on a track with irregularities; the value of displacement can be derived from the axle position in the assembly of the running gear and the vehicle velocity. Due to this fact, geometric filtering has a selective nature, depending on the vehicle wheelbases and velocity and on a differentiated efficiency, along the vehicle carbody and the movement behaviour, respectively.

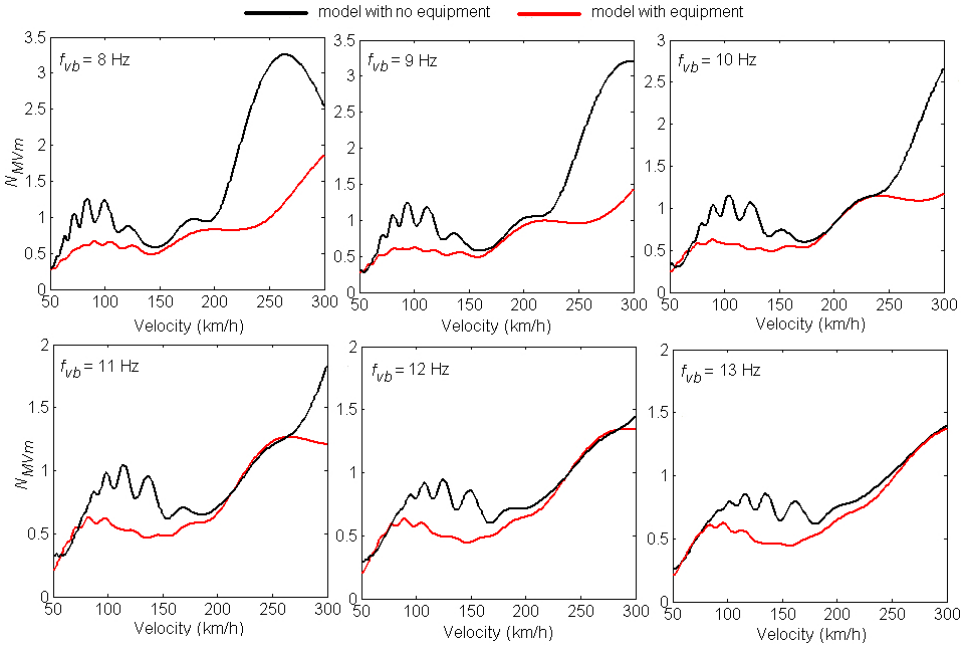

Fig. 5. The comfort index at carbody centre

One can notice the differences between the comfort index for the model without equipment and the same index for the model with equipment, which stand for an improvement in the ride comfort, thanks to the presence of equipment elements. This betterment varies within a large range, depending on the carbody bending

frequency f_{vb} and on the velocity. This improvement is shown in Fig. 6 as the percentage increase/decrease in the ride comfort at the carbody centre. An important increase in the ride comfort, which can reach up to 50–60%, is visible at high velocities, under the condition that the carbody bending frequency is lower than 10 Hz. For instance, the ride comfort is improved by 65% for $f_{vb} = 8$ Hz, at a speed of 255 km/h, thanks to the influence of equipment. While the carbody bending frequency rises ($f_{vb} = 12$ Hz or $f_{vb} = 13$ Hz), significant improvement in the ride comfort, reaching up to 20–30%, can be seen at velocities smaller than 150 km/h. For $f_{vb} = 12$ Hz, at a speed of 80 km/h, owing to the presence of equipment, the ride comfort improves by 31%. At high velocities, the improvement in the ride comfort does not exceed 10%.

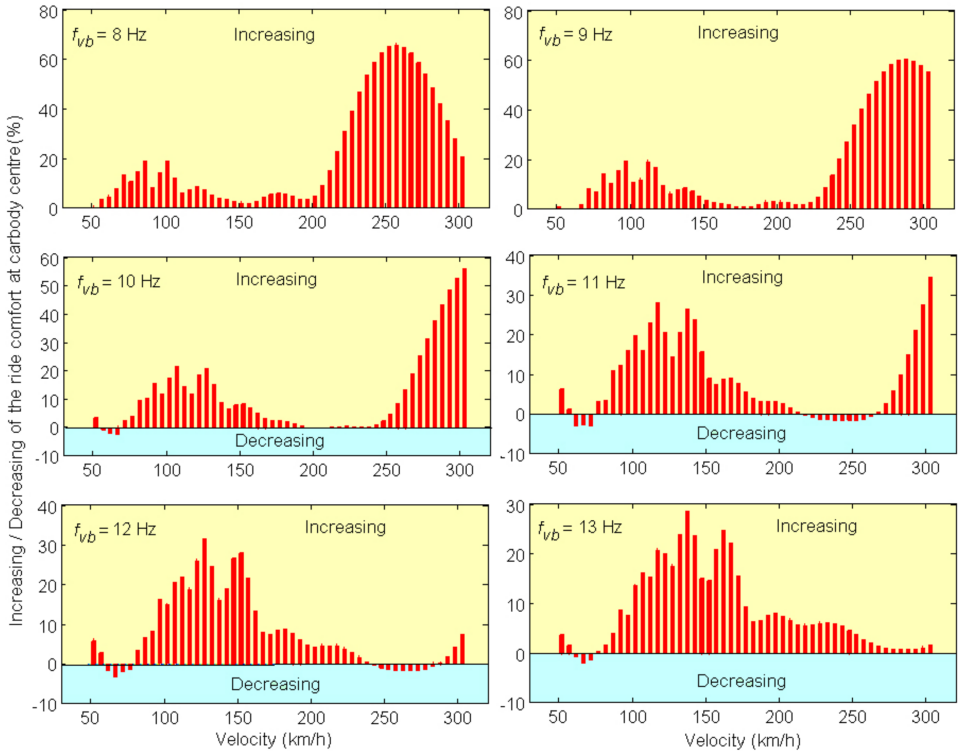

Fig. 6. The influence of the equipment on the ride comfort at the carbody centre

The diagrams in Fig. 7 and Fig. 8 depict the comfort index above the two bogies. Due to different behaviour of vibrations above the two bogies, there are differences between the comfort index above the front bogie and that above the rear bogie.

Nevertheless, a general trend is noticeable consisting in the increase in comfort index with the velocity. The raise is not continuous due to the geometric filtering

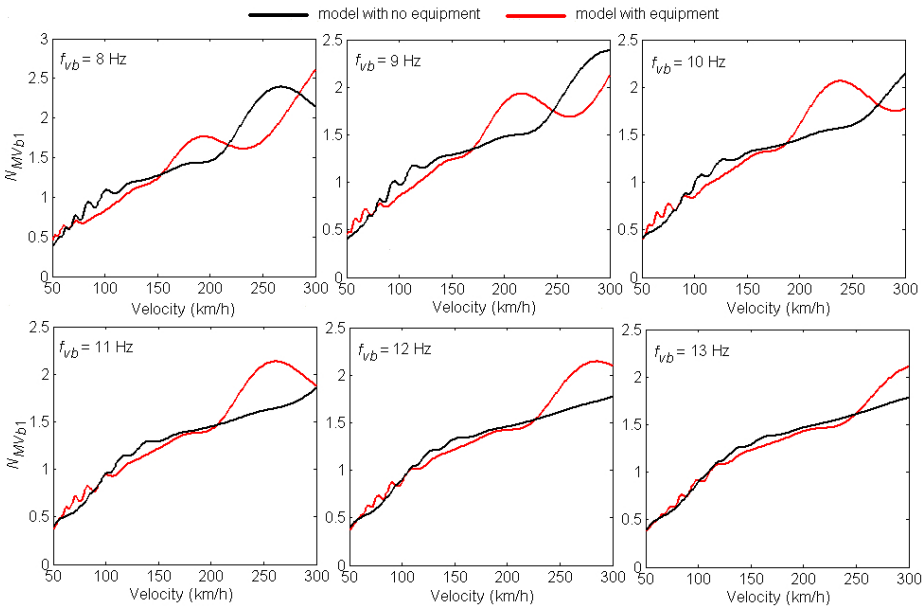

Fig. 7. The comfort index above the front bogie

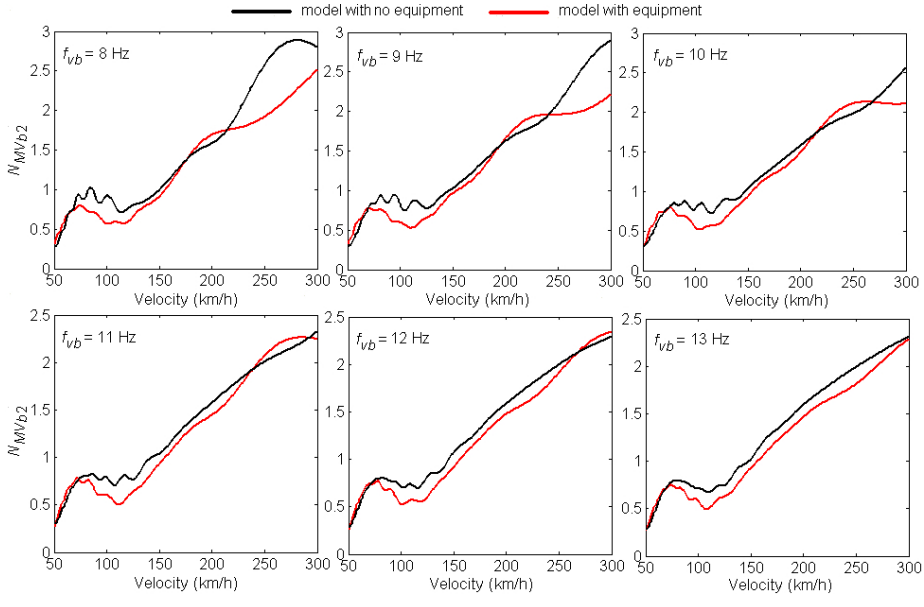

Fig. 8. The comfort index above the rear bogie

effect that has a lower efficiency here than at the carbody centre. The filtering due to the distance between bogies, occurring at the carbody centre, does not apply in this case.

www.czasopisma.pan.pl PAN POLSKA AKADEMIA NAUK www.journals.pan.pl

Unlike to the case of the carbody centre, where the ride comfort is improved thanks to the influence of equipment, there are large intervals of speed above the bogies where the comfort worsens. These intervals depend on the carbody bending frequency f_{vb}. The increase and the decrease of the ride comfort above the bogies, caused by the elements of equipment, is shown in Fig. 9 and Fig. 10. Considering the comfort index above the front bogie (Fig. 9), we can see that the most important growth of the ride comfort exceeding 20% is achieved at velocities higher than 250 km/h, for $f_{vb} = 8$ Hz or $f_{vb} = 9$ Hz. Practically, the largest increment (24%) occurs for $f_{vb} = 9$ Hz, at 250 km/h. When f_{vb} goes higher, the improvement in the ride comfort becomes smaller, under 10%. The decrease in the ride comfort is generally kept under 20% for $f_{vb} = 8$ Hz or $f_{vb} = 9$ Hz. At higher bending frequencies, the ride comfort will go down by more than 20%, reaching approximately 26% at 250 km/h for $f_{vb} = 11$ Hz.

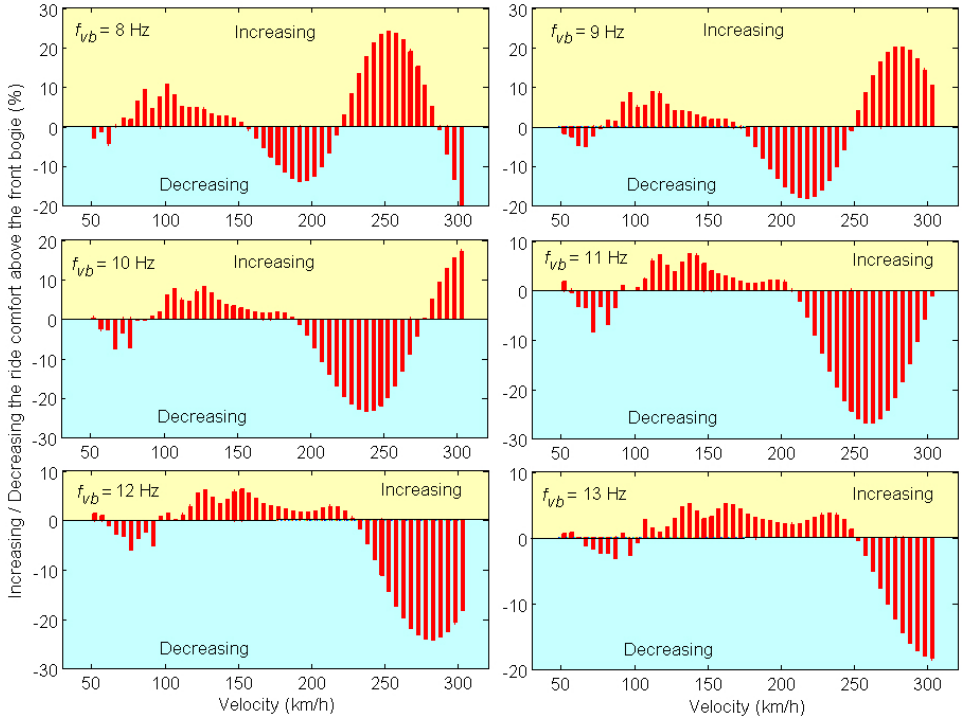

Fig. 9. The influence of the equipment on the ride comfort above the front bogie

There is also a significant enhancement in the ride comfort above the rear bogie (Fig. 10), for $f_{vb} < 11$ Hz. For example, an increase by approx. 23% in the ride comfort can be noticed, for $f_{vb} = 9$ Hz, at the speed of 300 km/h. For a higher f_{vb}, the growth in the ride comfort remains under 10%. The decrease in the ride comfort occurs in reduced intervals of speed, irrespective of the value of the carbody bending frequency, and is generally below 5%.

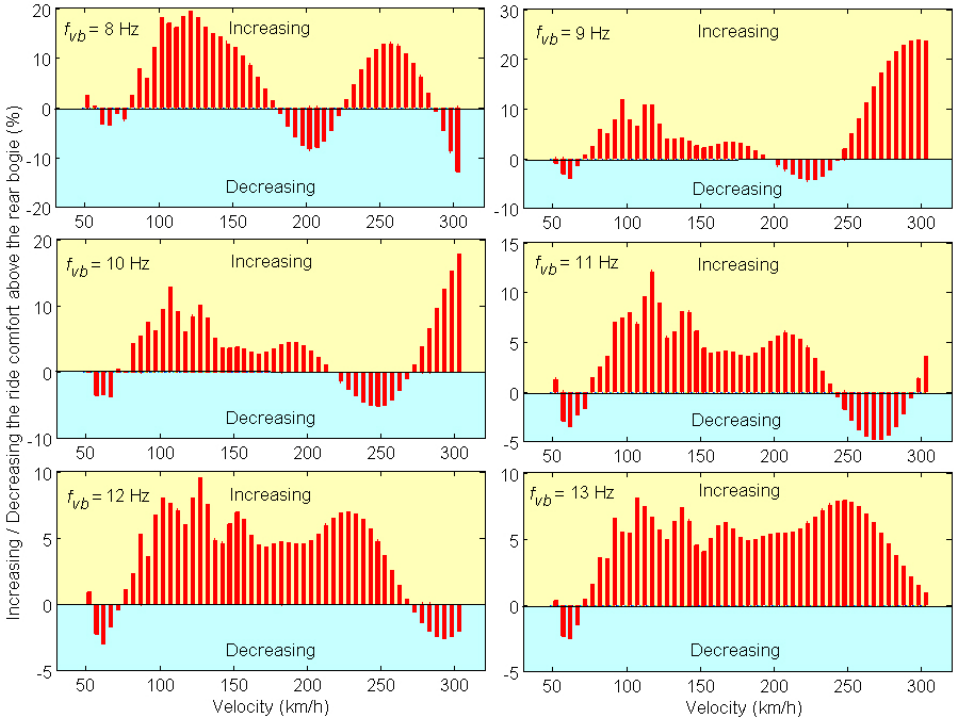

Fig. 10. The influence of the equipment on the ride comfort above the rear bogie

It is now interesting to see to what extent the ride comfort can be improved above the bogies by raising the value of ζ_e for the speed intervals where the comfort gets worse due to the presence of equipment. To this purpose, the diagrams in Fig. 11 can be used, as they show the comfort index above the two bogies for $f_{vb} = 11$ Hz, with ζ_e that takes the values of 0.025, 0.05 and 0.075.

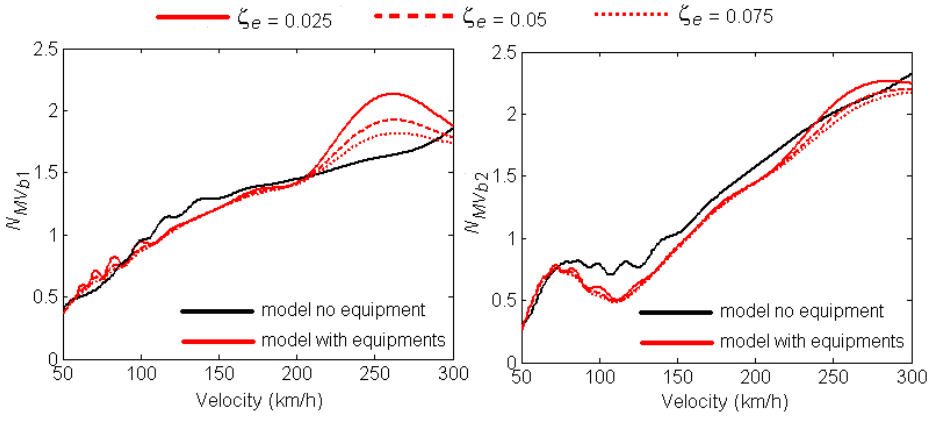

Fig. 11. The influence of the damping degree of the equipment suspension on the ride comfort

The increase in the damping ratio of the equipment results in the ride comfort improvement in all the cases above, for the entire speed interval. However, the most visible reduction in the comfort index is obviously noticed at high speeds. As an example, the comfort index decreases by 15% above the front bogie at the speed of 260 km/h and by 7% above the rear bogie, when ζ_e rises from 0.025 to 0.075.

4. Conclusions

This paper investigates the influence that the suspended equipment elements have on the ride comfort, based on the results from numerical simulations. The vehicle is represented by a rigid-flexible coupled model, out of which two distinct models are derived – the "model with no equipment" and the "model with equipment". Three reference points in the carbody are defined, such as at its centre and above the two bogies, where the ride comfort indices for the two models are calculated.

To analyse the influence of the equipment on the ride comfort, in correlation with velocity and the bending frequency of the carbody with no equipment, the ride comfort index was calculated in the carbody reference points, based on the models with six equipment elements, and the results were compared to the ones in the model with no equipment. In this way, an image of the change in the ride comfort, exclusively due to the influence of equipment, was obtained.

A generally valid observation is based on the fact that the ride comfort index rises with the speed, but this growth is not uniform, due to the geometric filtering effect. In terms of the influence of the equipment on the ride comfort, a separate discussion is needed for each of the carbody reference points. At the carbody centre, the results confirm an improvement in the ride comfort, but a substantial enhancement of up to 50–60% occurs at high speeds for carbody bending frequencies under 10 Hz. Above the bogies, this improvement (due to the presence of equipment) does not go beyond 25% at high speeds, provided that the carbody bending frequency is lower than 10 Hz. Additionally, there appear large speed intervals where the ride comfort gets worse because of the influence of equipment. The decline in the ride comfort generally remains under 20% if the carbody bending frequency is smaller than 10 Hz, but it can reach approx. 26% when carbody bending frequency is higher.

Manuscript received by Editorial Board, May 19, 2018;
final version, September 10, 2018.

References

[1] T. Tomioka, T. Takigami, and Y. Suzuki. Numerical analysis of three-dimensional flexural vibration of railway vehicle car body. *Vehicle System Dynamics*, 44:272–285, 2006. doi: 10.1080/00423110600871301.

www.czasopisma.pan.pl PAN POLSKA AKADEMIA NAUK www.journals.pan.pl

[2] C. Huang, J. Zeng, G. Luo, and H. Shi. Numerical and experimental studies on the car body flexible vibration reduction due to the effect of car body-mounted equipment. *Proceedings of the Institution of Mechanical Engineering Part F: Journal Rail and Rapid Transit*, 232(1):103–120, 2018. doi: 10.1177/0954409716657372.

[3] W. Sun, J. Zhou, D. Gong, and T. You. Analysis of modal frequency optimization of railway vehicle car body. *Advances in Mechanical Engineering*, 8(4):1–12, 2016. doi: 10.1177/1687814016643640.

[4] G. Yang, C. Wang, F. Xiang, and S. Xiao. Effect of train carbody's parameters on vertical bending stiffness performance. *Chinese Journal of Mechanical Engineering*, 29(6): 1120–1127, 2016. doi: 10.3901/CJME.2016.0809.090.

[5] G. Diana, F. Cheli, A. Collina, R. Corradi, and S.Melzi. The development of a numerical model for railway vehicles comfort assessment through comparison with experimental measurements. *Vehicle System Dynamics*, 38(3):165–183, 2002. doi: 10.1076/vesd.38.3.165.8287.

[6] H. Ye, J. Zeng, Q. Wang, and X. Han. Study on carbody flexible vibration considering layout of underneath equipment and doors. In: *4th International Conference on Sensors, Measurement and Intelligent Materials (ICSMIM 2015)*, pages 1177–1183, Shenzhen, China, 27–28 December, 2015.

[7] G. Luo, J. Zeng, and Q. Wang. Identifying the relationship between suspension parameters of underframe equipment and carbody modal frequency. *Journal of Modern Transportation*, 22(4):206–213, 2014. doi: 10.1007/s40534-014-0060-0.

[8] M. Dumitriu. Influence of suspended equipment on the carbody vertical vibration behaviour of high-speed railway vehicles. *Archive of Mechanical Engineering*, 63(1):145–162, 2016. doi: 10.1515/meceng-2016-0008.

[9] H.C. Wu, P.B. Wu, J. Zeng, N. Wu, and Y.L.Shan. Influence of equipment under car on carbody vibration. *Journal of Traffic and Transportation Engineering*, 12(4):50–56, 2012. (in Chinese)

[10] H.L. Shi, P.B. Wu and R. Luo. Coupled vibration characteristics of flexible car body and equipment of EMU. *Journal of Southwest Jiao Tong University*, 49(3): 693–699, 2014. (in Chinese).

[11] Y. Sun, D. Gong and J. Zhou. Study on vibration reduction design of suspended equipment of high speed railway vehicles. *Journal of Physics: Conference Series*, 2016, 744: Paper No. 012212.

[12] K.-I. Aida, T. Tomioka, T. Takigami, Y. Akiyama, and H. Sato. Reduction of carbody flexural vibration by the high-damping elastic support of under-floor equipment. *Quarterly Report of RTRI*, 56(4):262–267, 2015. doi: 10.2219/rtriqr.56.4_262.

[13] H. Shi, R. Luo, P. Wu, J. Zeng, and J. Guo. Influence of equipment excitation on flexible carbody vibration of EMU. *Journal of Modern Transportation*, 22(4):195–205, 2014. doi: 10.1007/s40534-014-0061-z.

[14] H.L. Shi, R. Luo, P.B. Wu, J. Zeng, and J.Y. Guo. Application of DVA theory in vibration reduction of carbody with suspended equipment for high-speed EMU. *Science China Technological Sciences*, 57(7):1425–1438, 2014. doi: 10.1007/s11431-014-5558-5.

[15] H.L. Shi, R. Luo, P.B. Wu, and J. Zeng. Suspension parameters designing of equipment for electric multiple units based on dynamic vibration absorber theory. *Journal of Mechanical Engineering*, 50(14):155–161, 2014 (in Chinese).

[16] W. Sun, D. Gong, J. Zhou, and Y. Zhao. Influences of suspended equipment under car body on highspeed train ride quality. *Procedia Engineering*, 16:812–817, 2011. doi: 10.1016/j.proeng.2011.08.1159.

[17] Y.Z. Nie, J. Zeng, and F.G. Li. Research on resonance vibration simulation method of high-speed railway vehicle carbody. In: *International Industrial Informatics and Computer Engineering Conference (IIICEC 2015)*, pages 1117–1121, Xi'an, Shaanxi, China, 10–11 January, 2015.

www.czasopisma.pan.pl PAN POLSKA AKADEMIA NAUK www.journals.pan.pl

[18] H. Shi and P. Wu. Flexible vibration analysis for car body of high-speed EMU. *Journal of Mechanical Science and Technology*, 30(1):55–66, 2016. doi: 10.1007/s12206-015-1207-6.

[19] C 116. Interaction between vehicles and track. RP 1, Power spectral density of track irregularities, Part 1: Definitions, conventions and available data. Utrecht, 1971.

[20] ENV 12299. Railway applications ride comfort for passengers measurement and evaluation, 1997.

[21] UIC 513 R. Guidelines for evaluating passenger comfort in relation to vibration in railway vehicle, International Union of Railways, 1994.

[22] J. Zhou, R. Goodall, L. Ren, and H. Zhang. Influences of car body vertical flexibility on ride quality of passenger railway vehicles. *Proceedings of the Institution of Mechanical Engineering Part F: Journal Rail and Rapid Transit*, 223(5):461–471, 2009. doi: 10.1243/09544097JRRT272.

[23] J. Zhou, W. Sun, and D. Gong. Analysis on geometric filtering phenomenon and flexible car body resonant vibration of railway vehicles. *Journal of Tongji University*, 37(9):1653–1657, 2009 (in Chinese).

[24] D. Gong, J. Zhou, and W. Sun. On the resonant vibration of a flexible railway car body and its suppression with a dynamic vibration absorber. *Journal of Vibration and Control*, 19(5):649–657, 2013. doi: 10.1177/1077546312437435.

[25] D. Gong, Y.J. Gu, and J.S. Zhou. Study on geometry filtering phenomenon and flexible car body resonant vibration of articulated trains. *Advanced Materials Research*, 787:542–547, 2013. doi: 10.4028/www.scientific.net/AMR.787.542.

[26] M. Dumitriu. Analysis of the dynamic response in the railway vehicles to the track vertical irregularities. Part I: The theoretical model and the vehicle response functions. *Journal of Engineering Science and Technology Review*, 8(4):24–31, 2015.

[27] M. Dumitriu. Analysis of the dynamic response in the railway vehicles to the track vertical irregularities. Part II: The numerical analysis. *Journal of Engineering Science and Technology Review*, 8(4):32–39, 2015.